Journal of Constructional Steel Research 148 (2018) 251–264

Contents lists available at ScienceDirect

Journal of Constructional Steel Research

Behaviour of restrained high strength steel columns at elevated temperature

Weiyong Wang [a,b,*], Linbo Zhang [a], Yong Ge [a], Lei Xu [a,c]

[a] College of Civil Engineering, Chongqing University, Chongqing 400045, China
[b] Key Laboratory of New Technology for Construction of Cities in Mountain Area (Ministry of Education), Chongqing University, Chongqing 400045, China
[c] Department of Civil and Environmental Engineering, University of Waterloo, 200 University Avenue West, Waterloo, ON N2L 3G1, Canada

ARTICLE INFO

Article history:
Received 1 April 2018
Received in revised form 23 May 2018
Accepted 24 May 2018
Available online xxxx

Keywords:
High strength Q460 steel
Column
Fire test
End restraint
Finite element analysis

ABSTRACT

High strength steel has been widely used in various types of structures due to its merits of high strength and good ductility. However, high strength steel structures are vulnerable to fire hazards as the strength and stiffness of the steel deteriorate rapidly at elevated temperature. Presented in this paper are the investigations on the behaviour of restrained high strength steel columns at elevated temperature obtained from full-scale fire tests and finite element analyses. In the fire tests, applied load and restraint stiffness are two key factors to be examined. Column responses such as the axial displacement, deflection at column middle height and axial force induced by thermal expansion associated with temperature evolution were reported. Column buckling and failure temperatures were determined based on the criteria of the axial displacemen t and lateral deflection of the specimens at elevated temperatures. The test results show that both the applied load and restraint stiffness have considerable influences on fire resistances of high strength steel columns. It was observed that the columns with only axial restraints failed by flexure buckling about the weak axis whereas the columns with both axial and rotational restraints and subjected to large magnitude of the applied load failed by flexural torsional buckling. Finite element analyses were conducted to simulate the fire responses of the test specimens and the obtained numerical results are found to be reasonably agree with the test data. Parametric studies via finite element analysis were carried out to quantitatively determine the effect of applied load, restraint stiffness and slenderness ratio on fire resistance of high strength steel columns.

1. Introduction

In recent years, high strength steels (HSS) are widely used in long-span structures and high-rise buildings primarily due to its merits of high yield strength and good ductility. For example, more than 400 tons of high strength steel are used in the construction of China National Stadium (so-called "Bird Net"), where the opening ceremony of 2008 Olympic Games was held [1]. As there is no a general consensus on the definition of HSS around the world, the yield limits adopted for categorizing HSS are different in various design standards. Generally, a type of steel is referred as high strength steel if its yield strength is not less than 460 MPa. In fact, one most common product of high strength steel in Far East is Q460 steel with the nominal yield strength of 460 N/mm^2.

In fire conditions, buckling of steel columns can occurs at a lower magnitude of load than that of at ambient temperature as the result of degradations of strength and stiffness at elevated temperatures [2,3]. In the case of local fire, the fire response or behaviour of a steel column with end restraints is quite different from that of a steel column without end restraints since the thermal expansion in the restrained steel column would result in an additional axial force in the heating phase [4]. In the cooling phase, the load applied on the restrained column may be transferred to the adjacent columns which have not experienced elevated temperature. Literature review [5] demonstrates that there are some fundamental researches on fire response of restrained steel columns, not only by testing, but also by finite element modelling. Li et al. [6,8] conducted a series of investigations on behavior of restrained steel column in fire with carrying out fire tests, finite element simulation and development of a practical design approach. It was found from the investigations that the axial restraint resulted in a lower buckling temperature for the restrained steel columns and the effects of axial restraint to the failure temperature were also related to the load ratio and the axial restraint stiffness ratio. Correia and Rodrigues [9] conducted fire tests on restrained steel columns and the results showed that increasing the stiffness of the adjacent structure members might not lead to a reduction of the critical temperature of a restrained steel column. Correia et al. [10] subsequently proposed a simple approach for fire design for steel columns with thermal elongation being restrained based on the results obtained from a parametric study using

* Corresponding author.
E-mail address: wywang@cqu.edu.cn (W. Wang).

https://doi.org/10.1016/j.jcsr.2018.05.022
0143-974X/

finite element software ABAQUS. Yang and Yang [11] carried out fire tests for ten unprotected restrained column specimens. The specimens were loaded by steady-state method and heated up to 500 °C. Craveiro et al. [12] conducted a series of experiments to investigate the behavior of restrained cold-formed steel built-up columns for both closed and open sections at elevated temperature. The results showed that the magnitudes of restraining stiffness and applied load are the important parameters influencing the fire behavior of the columns. In addition, it was found that the 350 °C of limit temperature for class 4 cross-sections stipulated in European code [13] is conservative.

From the aforementioned literature review, it was found that almost all the tests were carried out for mild steel or cold-formed steel columns. There are few publications reported on the investigation of the axially and rotationally restrained high strength steel columns at elevated temperature. It needs to point out the structural properties adopted for fire resistance design of steel structures in current design standards and specifications are not applicable for high strength steel structures since the deterioration of steel properties are different between mild and high strength steel [14]. To address this knowledge gap, a recent investigation, which includes an experimental test program and the corresponding finite element analysis, on the behaviour of high strength Q460 steel columns subjected to both fire and applied loading is presented in the following.

2. Experimental program

In order to investigate the fire response of restrained high strength steel columns, fire tests were carried out for the high strength steel columns with axially and rotationally end restraints in a fire furnace.

2.1. Specimen preparation

Eight column specimens were made of Q460 steel plate welded to a H-shape section of H200x195x8x8, in which four specimens were designed with axial end restraints with the length of 4.3 m, whereas the others are designed with both axial and rotational end restraints with the length of 4.48 m. The restraining stiffness at each end was provided by two H-shaped steel beams made of Q235 steel with the length of 3.2 m. Two cross-sections, namely H200x150x6x9 and H300x150x6.5x9 were fabricated for the beam to generated two different restraining stiffness. The mechanical properties of the test specimens and the restraining beams are obtained by the standard tension coupon test according to the ASTM A370 test protocol [15]. The test results are tabulated in Table 1.

For the specimens with the axial end restraints, the end conditions are hinge connected to the restraining beam to ensure the specimen ends can freely rotate about its weak axis. The end conditions of strong axis are seen as fixed and cannot rotate. For the specimens with both axial and rotational end restraints, extended end-plate connections were used to connect the column ends to the restraining beam in such a way both axial and rotational deformation at column ends are prevented. The aforementioned two types of end connections are illustrated in Fig. 1.

Different magnitudes of the applied load and restraining stiffness were considered in the tests. The axial restraint ratio β_a is defined as:

$$\beta_a = \frac{K_b}{K_c} = \frac{48E_bI_b}{l_b^3} \Big/ \frac{E_cA_c}{l_c} \tag{1}$$

Table 1
Material properties of steels by coupon tests.

Steel	Thickness	Yield strength	Ultimate strength	Elastic modulus
Q235	9 mm	285 MPa	415 MPa	2.10×10^5 MPa
Q460	8 mm	585 MPa	660 MPa	2.12×10^5 MPa

(a) (b)

Fig. 1. Connection between column specimen and restraining beam. (a) Hinged connection (b) Extended end-plate connection.

where K_b is the flexural stiffness associated with the mid-span deflection of the restraining beam; K_c is the axial stiffness of the column; I_b is the moment of inertia of the beam; A_c is the column cross sectional area; and l_b and l_c are the length of the beam and column, respectively.

The rotational restraint ratio is defined as:

$$\beta_r = \frac{K_{rb}}{K_{rc}} = \frac{12E_bI_b}{l_b} \Big/ \frac{3E_cI_c}{l_c} = \frac{4E_bI_bl_c}{E_cI_cl_b} \tag{2}$$

where K_{rb} is the rotational stiffness associated with the mid-span rotation of the restraining beam; K_{rc} is the end rotational stiffness of the column;

The load ratio R is expressed as:

$$R = N/N_{cr} \tag{3}$$

where N is the applied load placed on the column top end and N_{cr} is the ultimate load capacity of the column evaluated based on GB50017-2017 [16] at ambient temperature.

The detail information about the specimens is tabulated in Table 2.

2.2. Test set-up and measurements

The test specimens are heated in a fire furnace. The dimension of the furnace is 3.6 m wide, 4.6 m long and 3.3 m high. The maximum heat power generated by the furnace is 5 MW. Eight natural gas burners are installed in the furnace, and the furnace temperature was recorded by ten thermocouples placed in the test chamber over a fire test. The plan view of the furnace is shown in Fig. 2. During the fire test, the temperature readings in thermocouples (noted as FT1 ~ FT8) are used to compare with that of ISO-834 heating curve and the control system automatically adjusts corresponding fuel supply to maintain the furnace temperature with that of the heating curve.

A horizontal self-reaction loading system, consisting of a steel frame and two steel restraining beams (top beam and bottom beam), was designed to apply loading on the test specimen and provided desirable

Table 2
Parameters of the specimens.

Specimen No.	End restraint	Load (ratio)	β_a	β_r
S-1	Axial	0.25	0.45	0
S-2		0.40	0.45	0
S-3		0.25	0.17	0
S-4		0.40	0.17	0
S-5	Axial and rotational	0.20	0.45	36
S-6		0.20	0.17	14
S-7		0.36	0.45	36
S-8		0.38	0.17	14

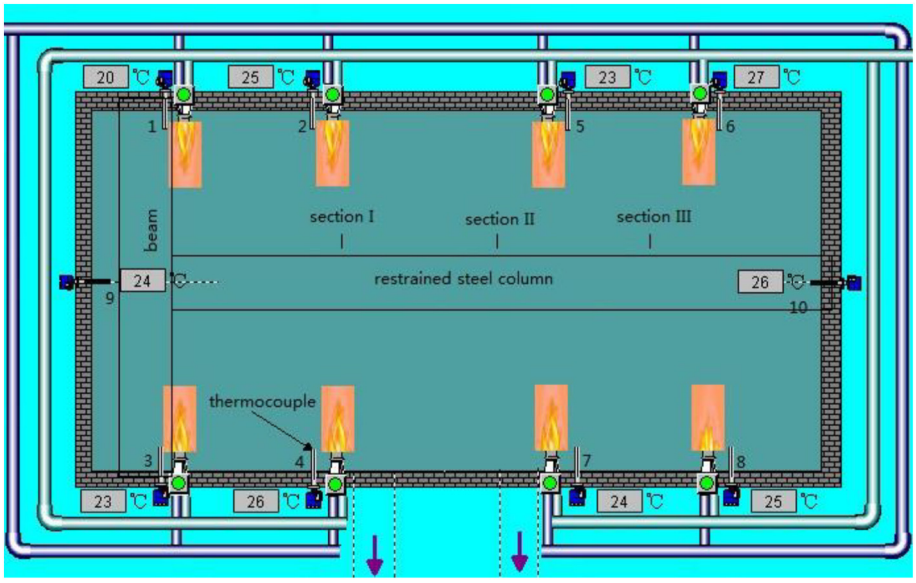

Fig. 2. Plan view of the fire furnace.

boundary conditions for specimen. The frame was horizontally placed on the top of furnace. Axial load applied on the test specimen by a horizontal hydraulic jack with capacity of 1000 kN. For the axially restrained columns, the top steel restraining beam provides an axial restraint on the test column as the temperature increases. For the axially and rotationally retrained columns, the top restraining beam provides not only the axial restraint but also the rotational restraint, and the bottom restraining beam only provides the rotational restraint to the column end. The axial restraint at the bottom of the specimen is provided by the stub column which supports the bottom restraining beam. The bottom beam hinged at the two ends is connected to frame with use of high strength steel bolts prior to the installation of the test column. After the installation of test specimen and top restraining beam, the bolts at the ends of top beam keep loose in order to apply the load on the restrained column. Until finishing applying load, the top restraining beam will be firmly connected to frame by tighten the high strength bolts. As the top beam was placed inside the furnace, it was protected with fire insulation in order to maintaining the restraining stiffness during the test. Shown in Fig. 3 is the layout of the test frame and the specimen set-up for the specimen with extended end-plate connections.

Thermocouples, strain gauges, and linear variable differential transformers (LVDTs) were used to record the thermal and structural responses of the test columns during the fire tests. The instrumentation of the test is shown in Fig. 3. Temperatures of the specimen were recorded by nine Type-K thermocouples, 2.0 mm in diameter. The thermocouples were located at the 1/3, 1/2 and 2/3 of the specimen length. Three strain gauges were placed to the short stub section connected the bottom restraining beam to evaluate the axial force generated in the restrained specimen. At locations of the top and mid-

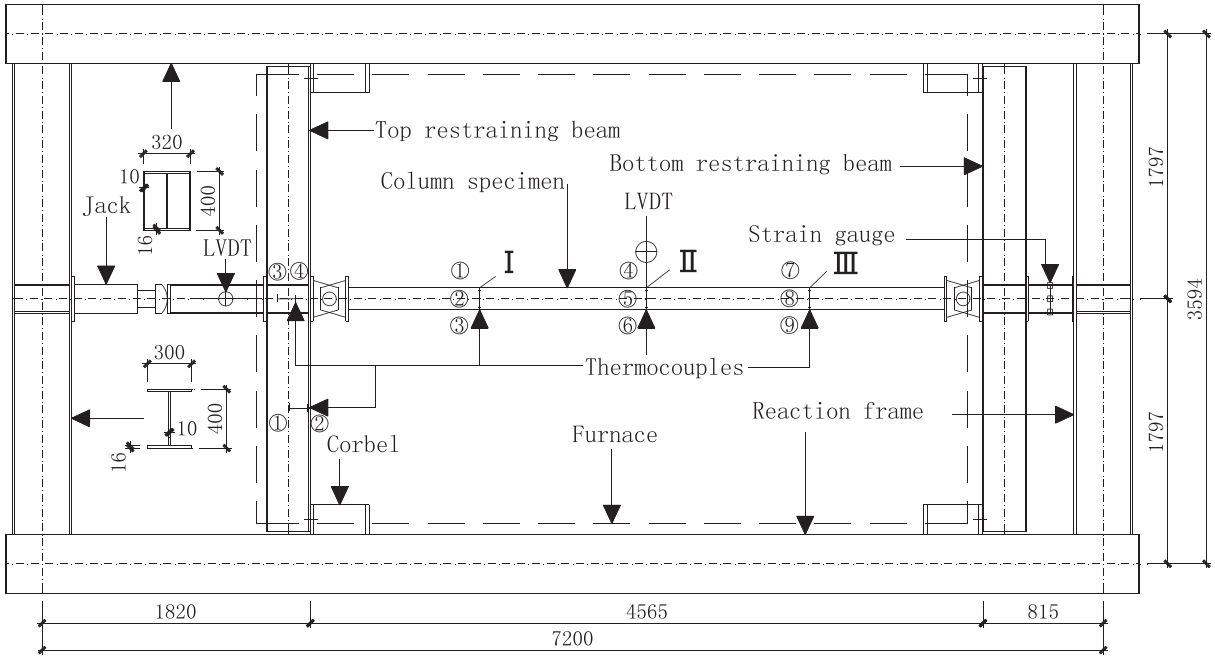

Fig. 3. Experimental loading system layout and specimen set-up.

height of the specimen, two LVDTS were installed to measure the axial displacement and lateral deflection of the specimen, respectively. The applied load on the test specimen was measured by a load cell mounted on the hydraulic jack.

2.3. Test procedure

The test process comprises of the following steps:

(1) The specimen was first placed into the loading frame and instrumentations on the specimen, including the thermocouple, strain gauges and LVDTs were subsequently installed.
(2) After all the test devices and instrumentation being checked and zeroed out, the applied loading from the hydraulic jack was increased to 10% of target load and kept for 5 min. The load was released to zero. This preloading process was repeated twice to ensure that all instruments exhibit linear variation with the load and all the readings returned to their starting value after the load was completely released. After preloading, the applied load was increased with a loading rate of 20kN/min until it reached to the target load. At this point, the top restraining beam will be firmly connected to the frame and the magnitude of the applied load was maintained throughout the duration of the fire test.
(3) The furnace was turned on and the furnace temperature was controlled in consistent with ISO-834 heating curve. If the axial displacement at the top end of specimen or the lateral deflection at the mid-height of the specimen reached the maximum range (l_c/100) or failure limit (l_b/20), respectively, the furnace was turned off and the applied load was released; and the test is terminated.

2.4. Test results

The test data obtained from the test was utilized to investigate the behavior of restrained high strength Q460 steel column subjected to elevated temperature. The effects of the applied load, and axial and rotational restraints on the behavior of high strength Q460 steel columns were evaluated through the comparison with thermal responses, structural responses, and failure patterns of the specimens.

2.4.1. Temperature evolution

The temperature evolution of the furnace, column specimens and top beams are plotted in Fig. 4. It can be seen that the furnace temperature was unable to match with that of ISO-834 curve initially due to the limitation of the maximum heat power of the furnace. However, a few (3–5) minutes later, the furnace temperature matched to ISO-834 curve closely. The column specimen was directly exposed to fire and its temperature increased quickly, which was attributed to the fact that the flange and web are thin and as well as the thermal conductively of steel are very high. The dispersion of temperatures across the column cross-section recorded by thermocouples showed it was less than 50 °C. Therefore, the effect of non-uniform distribution of the temperature in the column was negligible and the average temperature of the column was employed to represent the temperature of the specimen in the discussion of structural responses of specimens. During the test, the top restraining beam was wrapped with fire insulation and the corresponding temperature is relatively slow with the maximum temperature being only approximately 220 °C.

2.4.2. Axial displacement and lateral deflection

According to the previous research [7], for a restrained mild steel column in fire condition, the temperature at which the axial force reaches the maximum magnitude is defined as buckling temperature whereas the temperature associated with that when the axial force returns to its initial magnitude is defined as the failure temperature or critical temperature. When the axial displacement induced by thermal expansion approaches the maximum value, the axial force generated due to the axial restraint also reaches the maximum value.

Illustrated in Fig. 5 are the variations of the axial displacements of the specimens versus the time duration and specimen's temperature. As shown in the figure, the axial displacements increased gradually and with an abrupt drop when the maximum displacements are reached. From the fact that all the specimens failed at elevated temperature within 25 min, it can be concluded that the unprotected high strength steel columns are quite sensitive to fire. The failure temperature (T_1) of the specimens based on the abrupt change in axial displacements can be determined from Fig. 5 and they are tabulated in Table 3. It can also be found from Fig. 5 that the load ratio is also a critical factor to influence the fire resistance of the restrained column. At the same applied load ratio, taking an example of specimens S-1 and S-3, the specimen with higher axial restraining stiffness yields smaller axial displacement. It can be concluded that at the same applied load ratio, larger axial restraining stiffness would result in lower failure temperature of the columns. This can be attributed to the fact that the higher axial restraining stiffness would produce larger thermal force in the column. Consequently, the higher the axial force in the column would result in a lower the failure temperature.

It was observed that specimens S-1 and S-2 reached to a metastable state in post-buckling phase after the column specimens lost their capacities of resisting applied load due to buckling. In this phase, the applied load was resisted by the top restraining beam instead of the column. It should point out that this phenomenon was only observed for the column specimens with high axial restraining stiffness and relative lower load level, such as shown in S-1 and S-2. This phenomenon was not observed in columns with low restraining stiffness. In fact, this phenomenon was also observed in investigations of the restrained mild steel column by Franssen [17] and Wang [18].

The relationship between the lateral deflection at the mid-height of the specimen and the time duration and the temperature at mid-height of specimens is presented in Figs. 6(a) and (b), respectively. It can be seen from the figures that at initial stage of heating, the lateral deflection remains quite stable prior to reach the failure state. Abrupt increase of the lateral deflection was observed for all the specimens. The transition period from stable to failure state took a few seconds and the corresponding increase of the lateral flection was approximately about 200 mm. It 1 s also observed that some specimens experienced negative deflections in the initial stage of heating, such as specimen S-4. This may result from that the measurement of the deflection is located at the flange of the specimen, the negative deflection can be attributed to possible flange curling and torsion of the specimen in the initial heating stage.

In the case that the specimens are only subjected to the axial restraint, it is noticed from Fig. 5 that it took longer for specimen S-6 to reach the failure than that of specimen S-5 even though the both specimens were subjected to the same applied load. This is primarily due to the top restraining beam connected to S-5 was stiffer which yields a higher value of axial restraint ratio. Consequently, the higher value of axial restraint ratio results in a higher axial force associated with thermal expansion in the specimen as discussed in Section 2.4.3 and illustrated in Fig. 7. However, in the case that columns were subjected to both axial and rotational restraints, different from what was observed from specimens S-7 and S-8, it took a longer time for specimen S-7 to failure even though the axial restraint ratio of S-7 was greater than that of S-8. The reason of that is attributed to the higher value of the rotational restraint ratio associated with S-7 which enhanced the capacity of the specimen against the flexural torsional buckling comparing to that of specimen S-8.

2.4.3. Axial compressive force in the specimen

The variations of the axial force ratio, P/P_0, with the time duration and specimens' temperature are showed in Fig. 7, where P denotes the

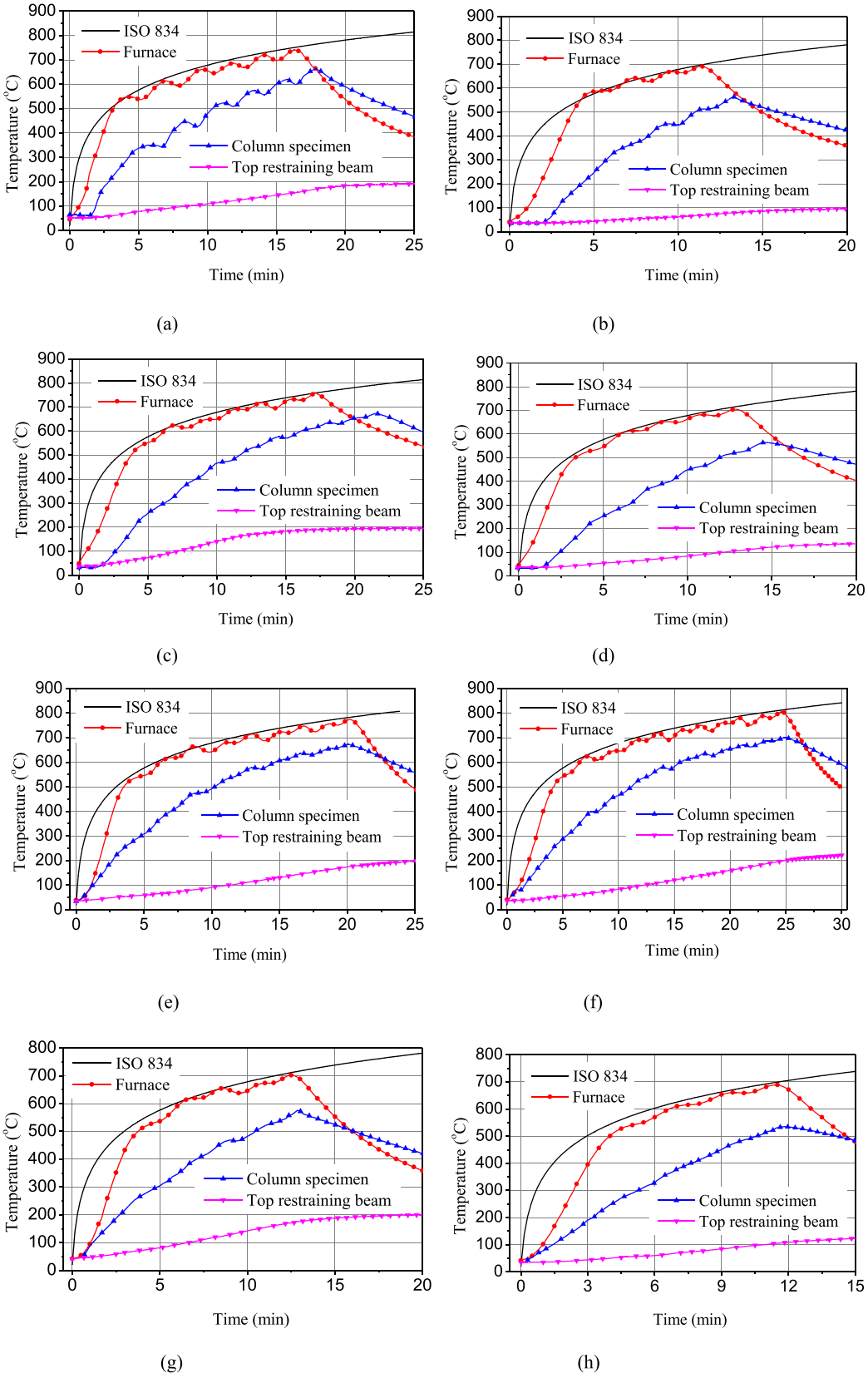

Fig. 4. Temperature distributions of furnace, specimen and top restraining beam. (a) Specimen S-1 (b) Specimen S-2. (c) Specimen S-3 (d) Specimen S-4. (e) Specimen S-5 (f) Specimen S-6. (g) Specimen S-7 (h) Specimen S-8.

axial force calculated based on the elastic modulus and strain of the stub column connected to the bottom end of the test specimen measured from the test; P_0 is the applied load on top of the specimen. The axial force induced by thermal expansion in the axially restrained column is greater for the column with the higher value of the axial restraint ratio and the lower value of the applied load ratio, which consequently

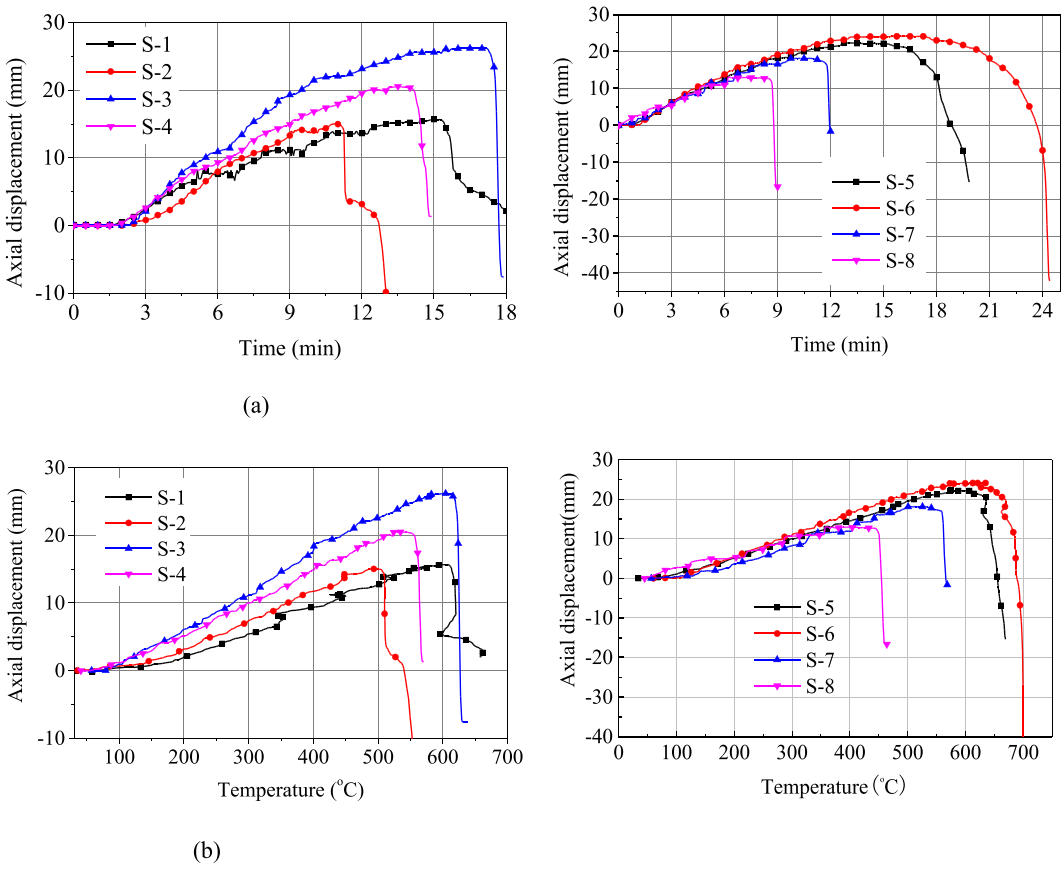

Fig. 5. Axial displacements of test specimens. (a) Relationship between axial displacement and time duration. (b) Relationship between axial displacement and specimen's temperature.

leads to a higher value of P/P_0, such as the case of S-1. The similar phenomenon is also observed for the specimen with both axial and rotational restraints and is clearly illustrated by specimen S-5 in the figure. The axial force in the column declined quickly after large lateral deformation was observed which signified the failure of the column.

Based on the aforementioned discussion, in addition to the failure temperature (T_1), defined based on the axial displacement of the specimen, the axial force of the specimen can be alternatively adopted to define the failure temperature (T_2) of the specimen. For the reason of comparison, in the failure temperatures T_1 and T_2 are presented in Table 3. It can be seen from the table there are some discrepancies among the failure temperatures T_1 and T_2, particularly for specimen S-8. The discrepancy can be attributed to the fact that the calculated axial force may not always that accurate by using strain obtained from the stub at the top of the specimen since the bottom beam could resist the axial force of the specimen in some degree.

2.4.4. Failure mode

Fig. 8 shows the failure modes of the test specimens. It is clearly that the failure modes of the specimens are influenced by the type of end restraints and magnitude of applied load. For the specimens S1 to S4, as the rotation about the weak axis of the specimens is not restrained, the failure mode is the flexural buckling about the weak axis of the specimens. For specimens with both axial and rotational restraints, in case of low magnitude of applied load, specimens S-5 and S-6, flexural buckling about the weak axis of the specimens was observed no matter the magnitudes of axial and rotational restraints. However, for the specimens subjected to high magnitude of applied load and with both axial and rotational restraints, S-7 and S-8, flexural torsional buckling was observed as indicated in Figs. 8 (g) and (h). The flexural torsional buckling can be attributed to the fact that the temperature distribution in these two specimens at the failure time may not be uniform. Considering the fact these two specimens were subjected to a higher applied load ratio and the corresponding flexural torsional buckling failure occurred at an earlier stage comparing to that of other specimens which were subjected to a lower applied load ratio. In the early stage of the test, the temperature increases quickly and the effects of non-uniform distribution can be more significant than that in the later stage. The non-uniform temperature distribution in the specimen may result in the stiffness distribution of the specimen is no longer double symmetrical. As for the other specimens, the flexural buckling failure happened in a longer fire exposure time due to the low applied load ratios and the corresponding temperature distribution at this stage is relatively uniform. Therefore, it appears that the failure mode of the specimens is more sensitive to the magnitude of applied load other than the magnitudes of axial and rotational restraints. Further investigations on the behaviour of the columns with the high applied load ratio and effect of non-uniform temperature distribution on the column failure mode are needed in future research.

Table 3
Critical temperature and failure time of the specimens.

Specimen No.	S-1	S-2	S-3	S-4	S-5	S-6	S-7	S-8
Buckling temperature/°C	606	493	582	530	607	617	512	412
Failure temperature T_1/°C	620	510	625	564	655	688	564	454
Failure temperature T_2/°C	652	550	603	558	669	699	560	356

2.5. Comparison with restrained mild steel columns

In order to investigate the difference of the fire responses between the restrained columns with high strength steel and mild steel. Test results of specimen RS97_4 in a fire test conducted by Tan et al. [19] was selected for the comparison with that of specimen S-2 in this investigation since both specimens have identical slenderness ratio of 96, applied

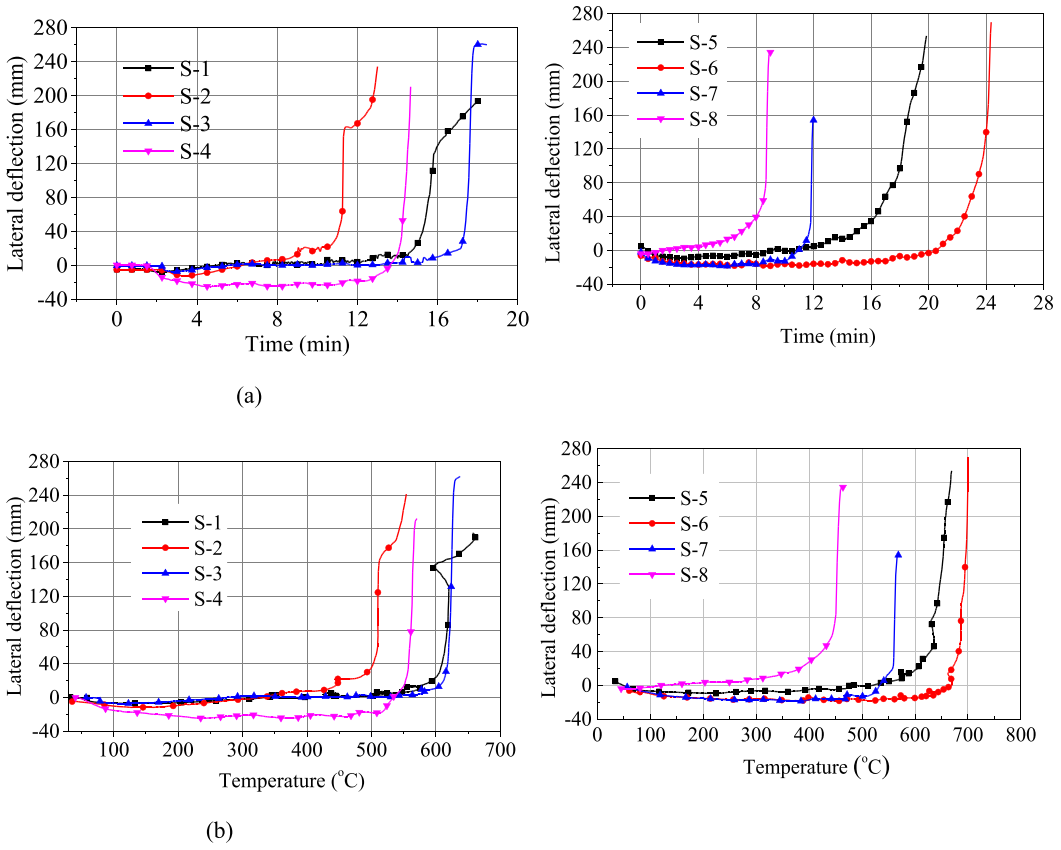

Fig. 6. Lateral deflection of test specimens. (a) Relationship between the lateral deflection and time duration. (b) Relationship between the lateral deflection and specimen's temperature.

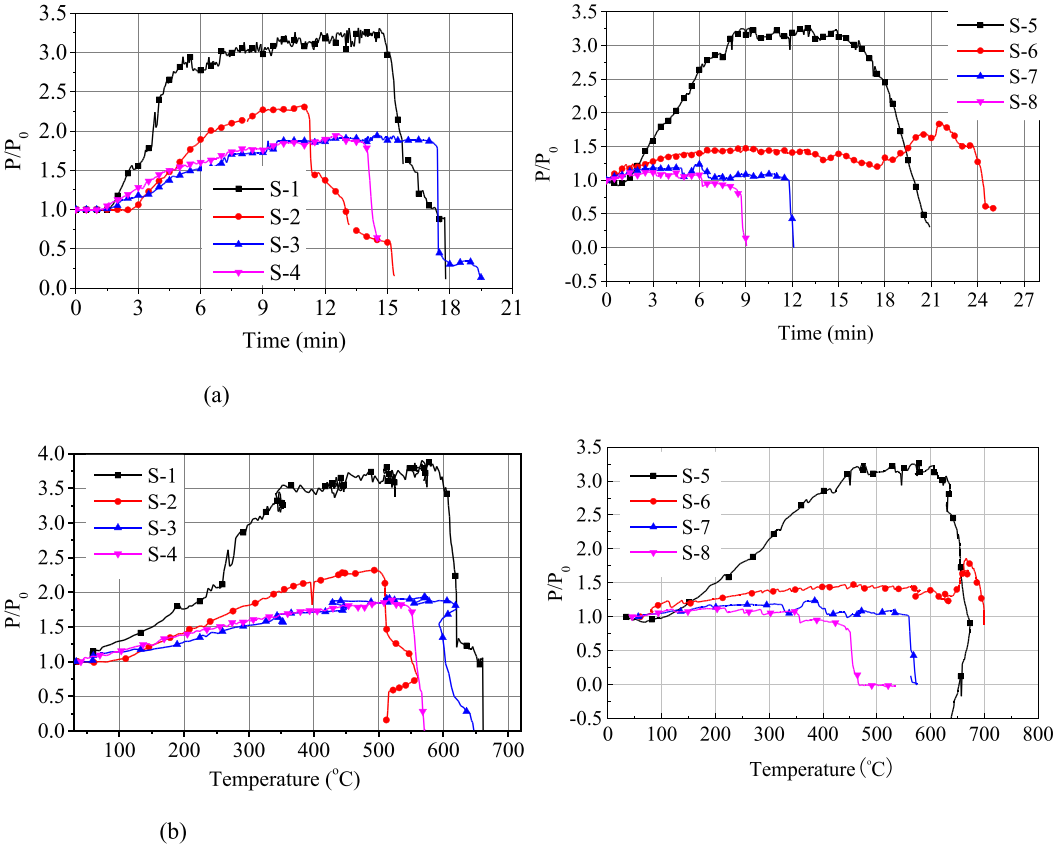

Fig. 7. P/P_0 of test specimens. (a) Relationship between the axial force ratio P/P_0 and time duration. (b) Relationship between the axial force ratio P/P_0 and specimen's temperature.

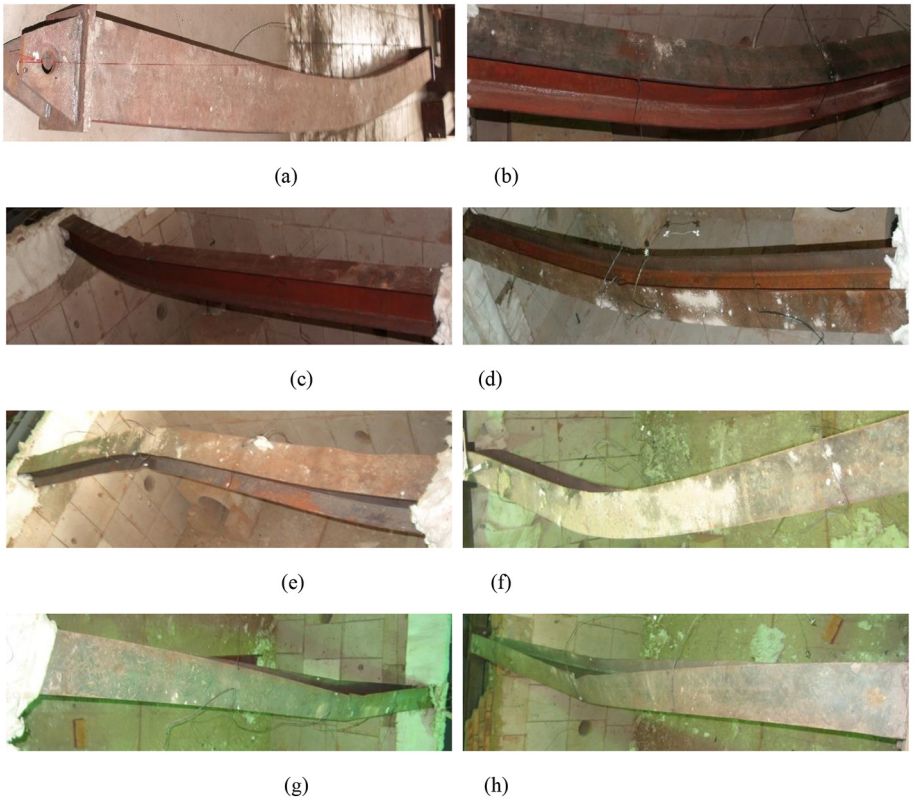

Fig. 8. Failure modes in test specimens. (a) Specimen S-1 (b) Specimen S-2. (c) Specimen S-3 (d) Specimen S-4. (e) Specimen S-5 (f) Specimen S-6. (g) Specimen S-7 (h) Specimen S-8.

load ratio of 0.5 and axial restraint stiffness ratio of 0.16. It can be seen from Fig. 9 there are significant differences between the maximum axial displacement and P/P_0 ratio because the length of RS97_4 is only 1.5 m, which is considerably shorter than that of S-2. However, it is noticed that P/P_0 ratios of the two specimens follow a close evolution in the early stage of the elevated temperature. It should point out that with the same test conditions, axially restrained column of Q460 steel generally exhibits much better fire resistance than that of mild steel. This conclusion also can be drawn by comparing the test results of this investigation with that of tests performed by Ali et al. [20]. The failure temperatures of axially restrained mild steel columns with slenderness of 98 ranged from 333 to 410 °C for applied load ratios and axial restraint stiffness ratios within a range of 0.4 and 0.6 and 0.1 and 0.2, respectively. Studies [7] on fire resistance of restrained steel columns have shown that increase of either the applied load or axial restraint stiffness would lead to a greater reduction in the failure temperature. For a column with the applied load ratio of 0.3, the axial restraint stiffness ratio of 0.34, and a slenderness of 51 similar to that of specimen S-7 in this investigation, the failure temperature of column HEA200-K128-L30 was approximately 515 °C as reported in [15], which is less than 564 °C obtained from this investigation for specimen S-7. Such observation can be explained that reduction factors of material properties for high strength steel Q460 at elevated temperature are greater than that of mild steel given in EC3 [13].

3. Finite element simulation

Fire test of full-scale specimen is costly and time consuming. Finite element simulation has been widely adopted as it can generate reasonable predictions for both thermal and structural responses of structures. The finite element software ANSYS was employed to perform fire response analysis of restrained high strength Q460 steel columns. Temperature dependent thermal and mechanical properties of the steel were adopted in the analysis and the restrained high strength Q460

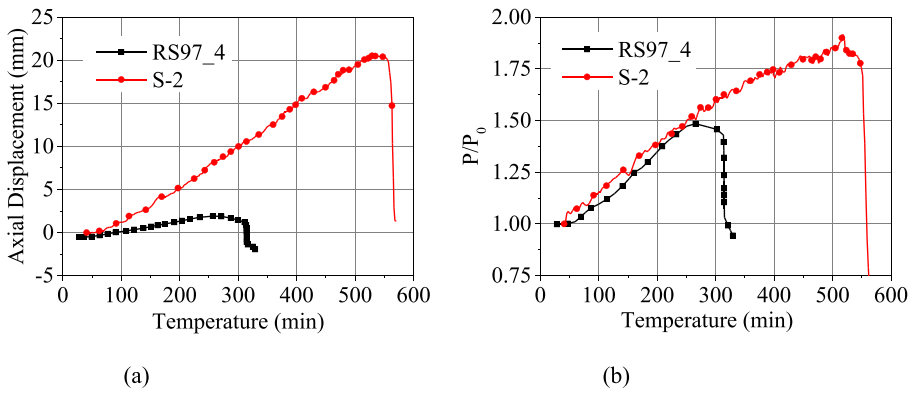

Fig. 9. Fire resistance comparison between mild and high strength restrained steel columns. (a) Axial displacement (b) Axial applied load ratio.

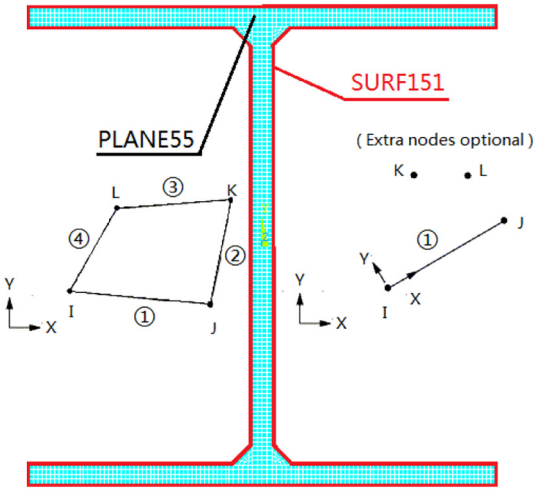

Fig. 10. FE model for thermal analysis.

steel columns with different magnitudes of the applied loads and boundary conditions were exposed to four-side fires in the simulation. Thermal and structural model of the column was established for finite element thermal and structural analysis, respectively.

3.1. Thermal analysis model

The analysis results from the three-dimensional finite element analysis of steel column subjected to standard ISO-834 fire indicated that the temperature in the steel column was uniformly distributed along the column length [21]. Therefore, a simple two-dimensional (2D) finite element analysis model to simulate the temperature distribution in cross-section was established. The steel column section was modeled by using element PLANE55 in ANSYS, which has four nodes with a single degree of freedom (temperature) at each node. Heat conduction can be simulated by specifying appropriate property for the thermal conductivity of the steel. In this investigation, the property specified in EC3 was adopted. To simulate the effect of heat convection and thermal radiation, the surface of PLANE55 2D thermal solid element was covered by SURF151 element, as depicted in Fig. 10. In the thermal analysis the recorded furnace temperature from the test was assigned to the exposed surface of SURF151 element. The value of convection coefficient was given in Chen [22] and the Stefan-Boltzmann radiation constant of $\sigma = 5.67 \times 10^{-8}$ W/(m^2 K^4) was used in the analysis. The thermal conductivity, convection coefficient, steel density, and heat specific, as per EC3, were plotted in Fig. 11a.

3.2. Structural analysis model

The mechanical model of the restrained steel column with two different column end boundary conditions and the applied load were shown in Fig. 12. Due to the large values of slenderness ratios, BEAM188 element was adopted to model the columns and connected restraining beams. BEAM188 element is Timoshenko beam element with both effects of shear deformation and large deformation being taken into accounted [23]. The pin-ended joint between the restraining beam and the column was simulated by using multipoint constraint element MPC184. Such element can also simulate a rigid joint element by using two nodes at same location and is capable of considering large deformation and nonlinear material behaviour. With using PLANET82 element, the cross-section mesh of the column specimen and restraining beam was shown in Fig. 13. The column and beam were both divided into 50 segments in their longitudinal direction. The constitutive

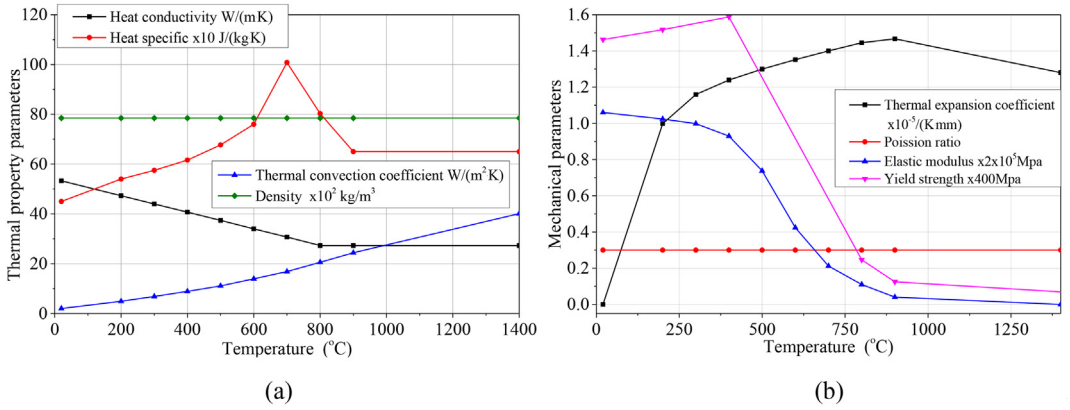

Fig. 11. Physics parameters of Q460 steel. (a) Thermal property parameters of Q460 steel (b) Mechanical parameters of Q460 steel

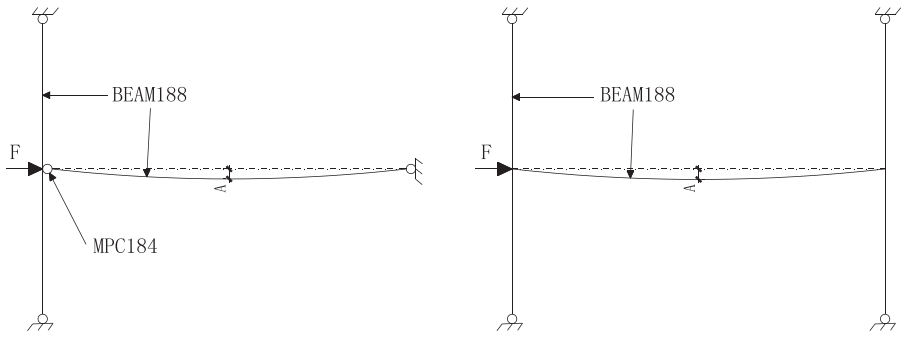

Fig. 12. Analytical model of ANSYS.

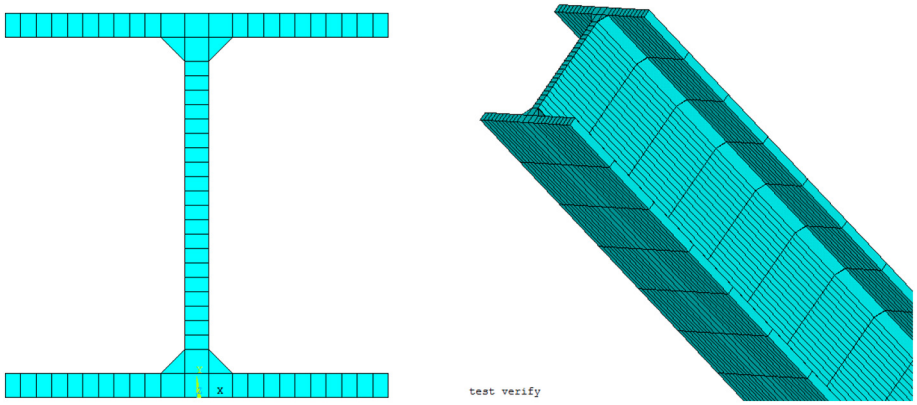

Fig. 13. FE model mesh.

models of Q460 and Q235 steel are bilinear ideal elastoplastic model, respectively. The corresponding mechanical properties at elevated temperature are presented in Fig. 11b, where the Poisson's ratio and thermal expansion coefficient are adopted from EC3. Elastic modulus and yield strength were determined in according to test results of Lange [24] and Wang et al. [14]. The variation of residual stress as a function of temperature proposed by Wang et al. [25] was adopted to calculate residual stress at elevated temperature. The geometric imperfection was incorporated into the model as following:

$$A = \frac{l}{1000}\sin\left(\frac{\pi x}{l}\right) \tag{4}$$

3.3. Model validation

The thermal analysis indicated that the maximum temperature located at the flange edges of the column section and the minimum temperature located at the intersection between the column web and flange. The maximum and minimum temperatures are presented in Fig. 14. It can be seen that the difference between these two temperatures is insignificant as the difference is less than 36 °C. Such trivial difference can be neglected because resulted variations of the yield strength and elastic modulus are very small. Therefore, the temperature in the steel column can be considered as uniformly distributed. For the eight fire tests presented in this study, the temperature evolution and structural response of the specimens were all simulated with the finite element analysis. The only differences in the model of each specimen were the applied load level and restraint ratio. Good agreements have been achieved between the numerical and experimental results in terms of axial displacement and deflection at the mid-height. For the purpose of the demonstration, thermal and structural analysis models were validated by comparison of the numerical results with the test results of specimen S-5 and S-6. Fig. 15 shows the column temperatures obtained by the finite element model and the test for section I, II and III shown in Fig. 3. It can be seen from the figure the numerical and experimental results are in good agreement.

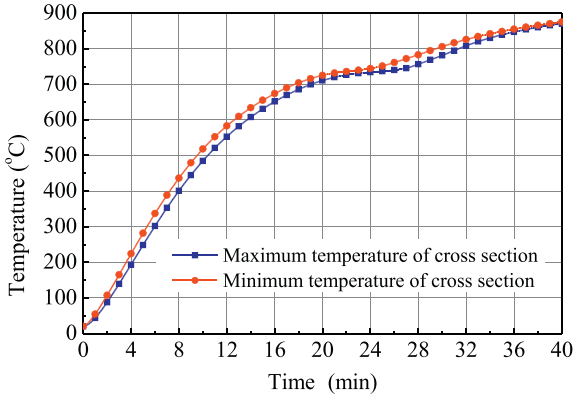

Fig. 14. Maximum and minimum temperatures of cross-section by thermal analysis.

In Fig. 16, Predictions on the axial displacements and lateral deflections of specimens S-5 and S-6 obtained by ANSYS are compared with the corresponding test results. In the test, if the column specimen experienced a large deformation, the test would be stopped immediately for the safety reason and avoidance of potential damages to the furnace. However, in the finite element analysis, the simulation would keep on going as long as the result convergence could be achieved. Thus, the predicted final deformation could exceed that was obtained from the test. Generally, the results obtained from the finite element modelling are less conservative than the tests. It can be found that the predicted axial displacements agrees well with the test results for the temperature up to 520 °C. For the lateral deflection at mid-height of the column, the predicted results agree well with test ones for the temperature up to 550 °C. The discrepancies of the predicted and test results for both the axial displacement and lateral deflection become to increase when the temperatures exceed the aforementioned values. The maximum difference of buckling temperature obtained from the prediction and test is approximately 50 °C The difference can be attributed to three possible reasons; one is that the local geometric imperfection was not considered in the analysis; and secondly the creep deformation of the steel column was not taken into consideration in the analysis; and the third reason for the discrepancy could be the variation in material properties at elevated temperatures, given that the assumptions for the material models are adopted from other studies [14,24] and not from a direct material testing of the specimen.

As for the failure mode, the results of finite element modelling indicated that flexural buckling about the weak axis is predominate failure mode for all eight specimens. This is true for all the specimens except S-7 and S-8 in which flexural torsional buckling was observed in the tests. As previously explained in Section 2.4.4, the flexural torsional buckling associated with S-7 and S-8 may result from the high applied load ratio and possible non-uniform temperature distribution in the specimens at the early stage of fire exposure. In the finite element modelling, the possible non-uniform temperature distribution was not accounted. Consequently, the failure mode obtained from the finite element modelling for S-7 and S-8 are flexural buckling about the weak axis.

4. Parametric study

To facilitate parametric studies, a simplified finite model of the column was established by replacing the restraining beam at each end of the column with an elastic spring as shown in Fig. 17. The spring

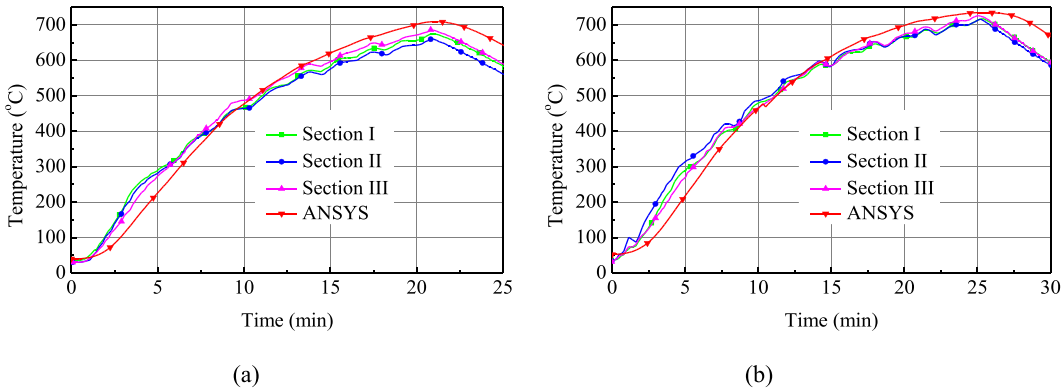

Fig. 15. Comparison of numerical and experimental results. (a) Specimen S-5 (b) Specimen S-6.

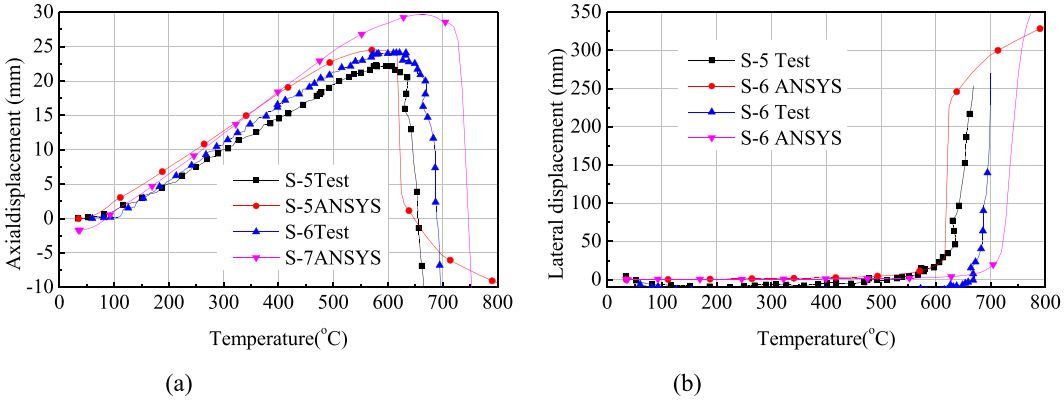

Fig. 16. Comparison of column responses between test and prediction. (a) Axial displacement (b) Deflection at mid-height.

element is COMBIN14 element, which has ability to simulating elastic springs associated with axial and torsional deformation in 1-D, 2-D, or 3-D models. The axial and torsional stiffness of COMBIN14 element were determined by that of the restraining beam.

The simplified finite model shown in Fig. 17 and analytical model shown in Fig. 12 were employed to simulate the fire test of specimen S-5. The results obtained from the both models are presented in Fig. 18 for the reason of comparison. In general, good agreements on both of the lateral deflection and axial displacement except minor deviations on the axial displacement when the temperature exceeds 700 °C. The analytical model is capable of simulating the fire test with both constant and variable end restraining stiffness which corresponding the elastic and inelastic behaviour of the restraining beam, respectively. The simplified model, however, is only applicable to the steel column with the constant end restraining stiffness. In the parametric study, the validated simplified finite element model was employed to perform the analysis of investigating effects of axial and rotational restraints, and as well as the applied load and column slenderness ratios on the buckling and failure temperatures. The effect of residual stress and global geometric imperfections were taken into accounted in the parametric study.

4.1. Axial restraint stiffness

The influence of the axial restraining stiffness on fire resistance of restrained mild steel column has been studied by many researchers. Fire tests on restrained steel column conducted by Rodrigues et al. [26] showed that the axial restraint could decrease the buckling temperature of the steel column; and the column with the larger the axial restraining stiffness the axial force would drop more slowly after the buckling of the column. The realistic values of the axial restraint ratio for structural steel frames in practice are approximately ranged from 0.004 to 0.05 [27].

The relationships between the axial force and temperature for different axial restraining stiffness were plotted in Fig. 19, in which the rotational restraint ratio β_r was taken as 0 and the applied load ratio is 0.5. Analysis results indicated that the buckling temperature and failure temperature of Q460 steel column reduced with the increase of axial restraining stiffness and the axial force decreased more slowly after the buckling for columns with larger axial restraining stiffness. When axial restraint ratio β_a reached to 10, the axial restraining spring undertook the majority the applied load after the buckling of the column which resulting in a higher failure temperature. It can be seen from Fig. 19 that the difference between buckling and failure temperature is greater for columns with larger axial restraining stiffness. Consequently, the post buckling stage stretches a longer range and the column can survive longer time duration in fire because of the lager axial restraining stiffness.

4.2. Rotational restraining stiffness

The FE analysis carried out by Valente and Neves [28] indicated that the failure temperature of steel column is higher for columns with larger rotational restraining stiffness until it reached to a certain magnitude. Wang et al. [7] reported that the axial force-temperature curves was similar to that with rotational restraint ratio of 2.0 when the rotational

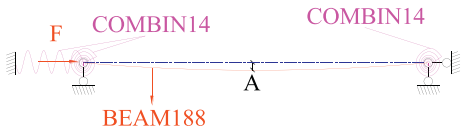

Fig. 17. FE model of restrained steel column for parametric analysis.

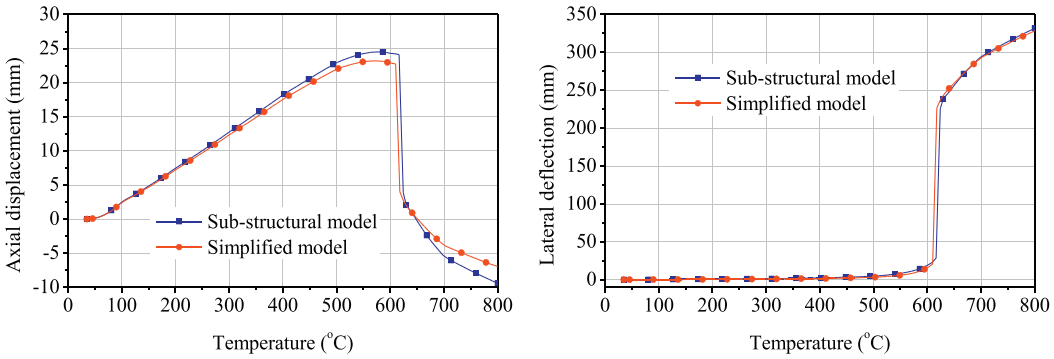

Fig. 18. Results comparison of analytical model and simplified model.

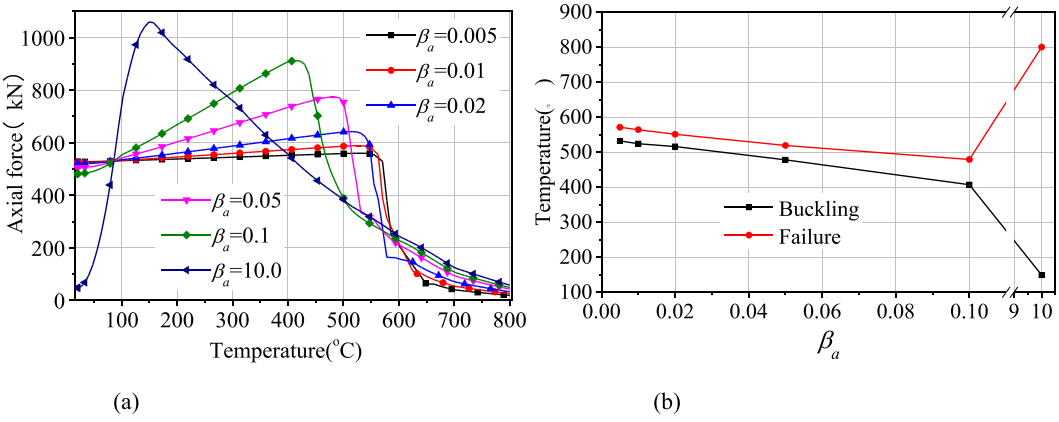

Fig. 19. The effect of axial restraint on fire behavior of the column. (a) Curves of axial force and temperature (b) Buckling and failure temperature.

restraint ratio (β_r) exceeded 2.0. In structural steel frames, the rotational restraint ratio for a column is not only related to the stiffness of the connected beams but also that of beam-to-column connections [29], which is often within the range of 0–1.0 [30]. The influence of the rotational restraint on Q460 steel column was presented in Fig. 20, where $\beta_a = 0.05$, $\rho_N = 0.5$ and $\lambda = 90$. From the analysis results, the limit of rotational restraint ratio on the mild steel column is also applicable for high strength Q460 steel column and the critical value of the rotational restraint ratio for Q460 steel column can be taken as 1.0. That is, if the rotational restraint ratio is less than 1.0, the higher rotational restraint ratio would result in the higher buckling temperature. When the rotational restraint ratio exceeds 1.0, the effect of the rotational restraint ratio on buckling temperature is not obvious.

4.3. Applied load ratio

Based on a study by Wang [18] on the fire resistance of restrained mild steel columns, it was found that that the axial force in the column would drop slowly when the applied load ratio is less than 0.5. However, the rate of the axial load decrease became more rapidly if the applied load ratio is greater than 0.5. The effects of applied load ratio on fire resistance of an axially restrained Q460 steel column from the parametric study were shown in Fig. 21, where $\beta_a = 0.05$, $\beta_r = 0$ and $\lambda = 90$. Both analysis and test results showed a similar trend which supports the aforementioned conclusion. It was also observed that from the figure that the increase of the applied load ratio, both of the buckling and failure temperatures decrease. This indicates that the higher of the applied

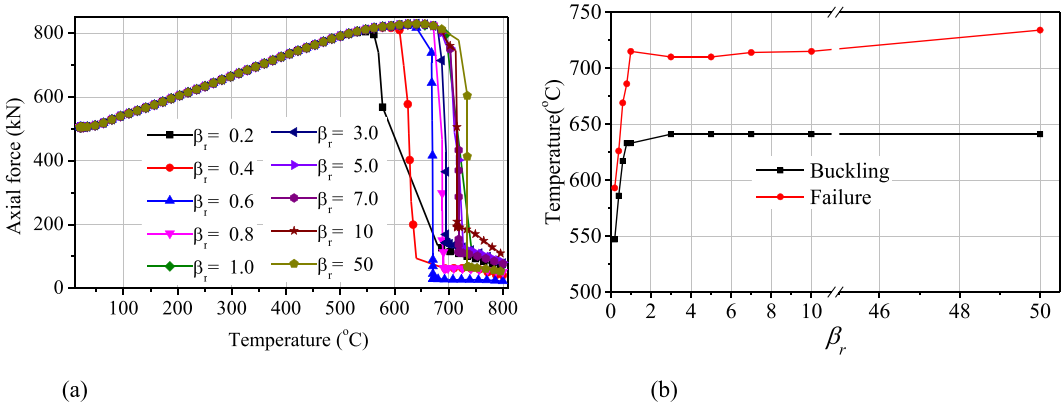

Fig. 20. The effect of rotational restraint on fire behavior of column. (a) Relationship of axial force and temperature (b) Buckling and failure temperature.

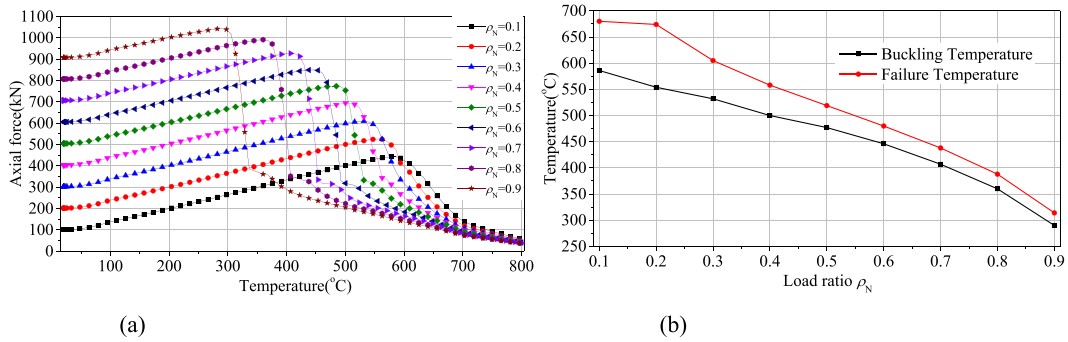

Fig. 21. Effects of applied axial load on fire resistance of the restrained Q460 steel column. (a) Curves of axial force and temperature (b) Buckling and failure temperature.

load ratio, the deterioration of the fire resistant of Q460 steel column would be more severe. In addition, the drop of the axial force after column buckling becomes more rapidly and the difference between the buckling and failure temperatures comes to be smaller with higher applied load ratio. This may explain the reason of the axial restraint delays the failure of Q460 steel column when the applied axial load is relatively small.

4.4. Column slenderness ratio

Fig. 22 shows the effects of column slenderness ratio on the fire resistance of restrained Q460 steel column with $\beta_a = 0.05$, $\beta_r = 0$ and $\rho_N = 0.5$. It is evidenced that both of the buckling and failure temperatures decrease with the increase of the slenderness ratio and the slenderness ratio has a minor influence on the failure temperature when the ratio is less than 60. When the slenderness ratio is less than 60, the drop rate of the axial force becomes slower as the decrease of the slenderness ratio which results in larger differences between the buckling and failure temperatures. When the slenderness ratio ranges between 60 and 90, the effect of the slenderness ratio on the difference between the buckling and failure temperatures is very minor. However, the difference becomes to increase as the increase of the slenderness ratio when the ratio exceeds 90.

5. Conclusions

Based on the aforementioned experimental and numerical investigations on the fire behavior of restrained high strength Q460 steel columns, the following conclusions can be drawn:

(1) Restrained high strength Q460 steel columns without fire protection are quite sensitive to the elevated temperature even though the applied axial load is relatively small and the columns can only survive approximately 20 min in fire scenario of ISO-834.
(2) Applied load ratio is a critical factor to influence the fire resistance of the restrained high strength steel column.
(3) For the columns subjected to the same magnitude of the applied load, the one with the larger axial restraining stiffness would result in a lower buckling temperature. In addition, the columns with the lager axial restraining stiffness, the corresponding post buckling stage is prolonged and the columns can survive a longer in fire duration.
(4) At the same condition, the fire performance of the restrained high strength steel columns is better than that of mild steel columns.
(5) When the rotational restraint ratio is less than 1.0, the higher value of the rotational restraint ratio would result in a higher buckling temperature. But the efficiency of the rotational restraint ratio on buckling temperature becomes less effective if the ratio exceeds 1.0.
(6) For the axially restrained high strength steel column with smaller slenderness ratio, the axial force drops slowly after the column bucked which consequently results in a larger difference between the buckling and failure temperatures for the column with slenderness ratio less than 60. There is a minor influence on the difference between the buckling and failure temperatures when the slenderness ratio ranged between 60 and 90. Once the slenderness ratio exceeds 90, the difference between the buckling and failure temperatures increases as the increase of the slenderness ratio.

Acknowledgement

The authors wish to acknowledge the supports of the Natural Science Foundation of China (51678090) and Chongqing University to the fourth author to the status of visiting professor. Any opinions, findings, and conclusions or recommendations expressed in this paper are those of the authors and do not necessarily reflect the views of the sponsors.

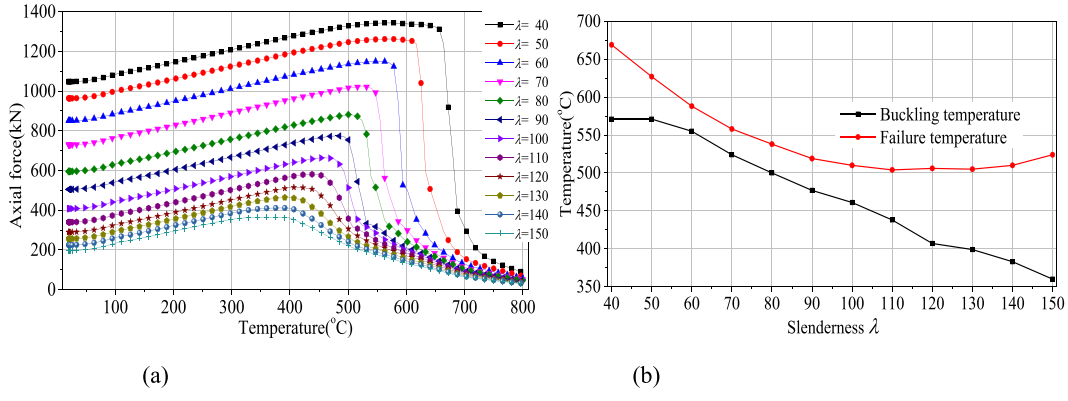

Fig. 22. Effects of slenderness ratio on fire resistance of restrained 460 steel column. (a) Curves of axial force and temperature (b) Buckling and failure temperature.

References

[1] W.Y. Wang, K. Wang, V.K. Kodur, B. Wang, Mechanical properties of high strength Q690 steel at elevated temperature, J. Mater. Civ. Eng. 30 (5) (2018), 04018062. .

[2] Y. Li, W.G. Li, X.H. Zhang, et al., Modeling of temperature dependent yield strength for stainless steel considering nonlinear behaviour and the effect of phase transition, Constr. Build. Mater. 159 (2018) 147–154.

[3] S.G. Fan, L.L. Jia, X. Lyu, et al., Experimental investigation of austenitic stainless steel material at elevated temperatures, Constr. Build. Mater. 155 (2017) 267–285.

[4] G.B. Lou, C.H. Wang, J. Jiang, al. Yet, Fire tests on full-scale steel portal frames against progressive collapse, J. Constr. Steel Res. 145 (2018) 137–152.

[5] J.P.C. Rodrigues, F.C.Teixeira Gomes, Fire Resistance Tests on Steel Columns, a Summary Overview, World Congress on Housing, 2012.

[6] G.Q. Li, P.J. Wang, Y.C. Wang, Behaviour and design of restrained steel column in fire, part 1: fire test, J. Constr. Steel Res. 66 (8–9) (2010) 1138–1147.

[7] P.J. Wang, G.Q. Li, Y.C. Wang, Behaviour and design of restrained steel column in fire: part 2: parameter study, J. Constr. Steel Res. 66 (8–9) (2010) 1148–1154.

[8] P.J. Wang, G.Q. Li, Y.C. Wang, Behaviour and design of restrained steel column in fire: part 3: practical design method, J. Constr. Steel Res. 66 (11) (2010) 1422–1431.

[9] A.J.P.M. Correia, J.P.C. Rodrigues, Fire resistance of steel columns with restrained thermal elongation, Fire Saf. J. 50((2012) 1–11.

[10] A.J.P.M. Correia, J.P.C. Rodrigues, F.C.T. Gomes, A simplified calculation method for fire design of steel columns with restrained thermal elongation, Comput. Struct. 116((2013) 20–34.

[11] K.C. Yang, F.C. Yang, Fire performance of restrained welded steel box columns, J. Constr. Steel Res. 107((2015) 173–181.

[12] H.D. Craveiro, J.P.C. Rodrigues, L. Laím, Experimental analysis of built-up closed cold-formed steel columns with restrained thermal elongation under fire conditions, Thin-Walled Struct. 107((2016) 564–579.

[13] European committee for standardization (ECS), Eurocode3: Design of Steel Structures, Part 1.2: General Rules—Structural Fire Design, EN1993-1-2, Brussels 2005.

[14] W.Y. Wang, B. Liu, V.K.R. Kodur, Effect of temperature on strength and elastic modulus of high strength steel, J. Mater. Civ. Eng. 25 (2) (2013) 174–182.

[15] American Society for Testing and Materials International (ASTM), Designation: A370-09 Standard Test Methods and Definitions for Mechanical Testing of Steel Products, West Conshohocken, PA 2009.

[16] Standardization Administration of the People's Republic of China (SAC), Code for Design of Steel Structures, GB50017-2017 China Standard Press, Beijing, 2017.

[17] J.M. Franssen, Failure temperature of a system comprising a restrained column submitted to fire, Fire Saf. J. 34 (2000) 191–207.

[18] Y.C. Wang, Post buckling behaviour of axially restrained and axially loaded steel columns under fire conditions, J. Struct. Eng. 130 (3) (2004) 371–379.

[19] K.H. Tan, W.S. Toh, Z.F. Huang, G.H. Phng, Structural responses of restrained steel columns at elevated temperatures, part 1: experiments, Eng. Struct. 29 (8) (2007) 1641–1652.

[20] F. Ali, P. Shepherd, M. Randall, I.W. Simms, et al., The effect of axial restraint on the fire resistance of steel columns, J. Constr. Steel Res. 46 (1–3) (1998) 305–306.

[21] V.K.R. Kodur, M.M.S. Dwaikat, Response of steel beam-columns exposed to fire, Eng. Struct. 31 (2) (2009) 369–379.

[22] J. Chen, Measurement and Analysis on Residual Stress in GJ Steel Welded I-Shaped Cross-Sectional Member, Master's Degree Thesis Chongqing University, Chongqing, 2010.

[23] L.L. Zhang, P.J. Wang, Simplified analysis method for catenary action of restrained cellular steel beams at elevated temperature considering strain reversal, Fire Saf. J. 95 (1) (2018) 145–159.

[24] J. Lange, N. Wohlfeil, Examination of the mechanical properties of steel S460 for fire, J. Struct. Fire Eng. 1 (3) (2010) 189–204.

[25] W.Y. Wang, G.Q. Li, Y. Ge, Residual stress study on welded section of high strength Q460 steel after fire exposure, Adv. Steel Constr. 11 (2) (2015) 150–164.

[26] J.P. Rodrigues, I.C. Neves, J.C. Valente, Experimental research on the critical temperature of compressed steel elements with restrained thermal elongation, Fire Saf. J. 35 (2) (2000) 77–98.

[27] Y.C. Wang, Effects of structural continuity on fire resistant design of steel columns in non-sway multi-storey frames, Fire Saf. J. 28 (2) (1997) 101–116.

[28] J.C. Valente, I.C. Neves, Fire resistance of steel columns with elastically restrained axial elongation and bending, J. Constr. Steel Res. 52 (3) (1999) 319–331.

[29] X.H. Qiang, N.D. Wu, X. Jiang, Y.F. Luo, Experimental and theoretical study on high strength steel extended endplate connections after fire, Int. J. Steel Struct. (2018) https://doi.org/10.1007/s13296-018-0020-3.

[30] F. Ali, A. Nadjai, D. Talamona, Effect of rotational restraint on performance of steel columns in fire, J. Appl. Fire Sci. 13 (1) (2004) 21–24.